L I V	1 2 4 2 1	WILEY	Dispatch: 10.12.13	CE: Prema
Journal Code	Manuscript No.		No. of pages: 12	PE: Prasanna

Liver International ISSN 1478-3223

ORIGINAL ARTICLE

FoxO3a modulation and promotion of apoptosis by interferon-α2b in rat preneoplastic liver

Juan P. Parody[1], Maria P. Ceballos[1], Ariel D. Quiroga[1], Daniel E. Frances[1], Cristina E. Carnovale[1], Gerardo B. Pisani[2], Maria L. Alvarez[1] and Maria C. Carrillo[1,2]

1 Instituto de Fisiología Experimental, Consejo Nacional de Investigaciones Científicas y Técnicas (CONICET), Rosario, Argentina
2 Area de Morfología, Facultad de Ciencias Bioquímicas y Farmacéuticas, Universidad Nacional de Rosario, Rosario, Argentina

Keywords
hepatocarcinogenesis – MAPK – oxidative stress – PUMA – rats

Correspondence
María Cristina Carrillo, PhD, Instituto de Fisiología Experimental, Consejo Nacional de Investigaciones Científicas y Técnicas (CONICET), Suipacha 570, S2002LRL Rosario, Argentina
Tel: +54 341 4305799
Fax: +54 341 4399473
e-mail: carrillo@ifise-conicet.gov.ar

Received 4 January 2013
Accepted 21 November 2013

DOI:10.1111/liv.12421

Abstract

Background: FoxO3a, a member of the FOXO family of transcription factors, is expressed in adult liver and modulates the expression of genes involved in apoptosis. FoxO3a is post-translationally regulated, negatively by PI3K/Akt and MAPK/Erk and positively by oxidative stress/JNK pathways. In previous works, we have demonstrated that interferon-α2b (IFN-α2b) induces apoptosis of hepatic preneoplastic foci through the production of reactive oxygen species (ROS). *Aims:* To investigate the post-translational signal events triggered by the oxidative stress induced by IFN-α2b and the modulation of FoxO3a transcriptional activity during these events in rat preneoplastic liver. *Methods:* Adult male Wistar rats were subjected to a two-phase model of hepatocarcinogenesis. A group of animals received IFN-α2b and another group received IFN-α2b and ascorbic acid (ASC), by intraperitoneal injection. Lipid peroxidation, immunohistochemistry, immunoblotting, co-immunoprecipitation and sqRT-PCR assays were performed to explore the role of ROS, JNK, Akt, Erk, FoxO3a, β-catenin and PUMA in the IFN-α2b-mediated apoptotic mechanism. *Results: In vivo* IFN-α2b treatment induced endogenous production of ROS which activated JNK. IFN-α2b blocked the activation of Akt and Erk, avoiding FoxO3a activity repression. Activated JNK was responsible for the nuclear translocation and transcriptional activity of FoxO3a which positively modulated the expression of PUMA, a proapoptotic player. In addition, nuclear FoxO3a competed for the nuclear β-catenin associated to TCF, inhibiting the canonical Wnt signalling pathway. *Conclusions:* The data presented here propose a model in which *in vivo* IFN-α2b treatment induces nuclear translocation and transcriptional activity of FoxO3a, triggering the mitochondrial apoptotic pathway in hepatic preneoplastic foci.

Hepatocellular carcinoma (HCC) is one of the most common malignancies worldwide (1). Hepatitis B or C viral infections are main risk factors for HCC development (2). Because of the increasing incidence of hepatitis C virus infection in the western world, HCC is becoming a growing health problem in developed countries (3).

The O subclass of the Forkhead family of transcription factors, or FOXO, plays important roles in different cellular processes including apoptosis, proliferation and protection from oxidative stress. There are four members of the FOXO family in mammals (4, 5), among these members, FoxO3a expression pattern is ubiquitous in murine adult tissue and is highly expressed in developing liver (4, 6). FOXO proteins are post-translationally regulated by several biochemical signalling cascades. They are direct substrates of the protein kinase Akt and are negatively regulated in response to cellular stimulation by growth factors or insulin (7–12). In this regard, phosphorylation of FOXO by Akt induces nuclear exclusion and sequestration in the cytosol mediated by 14-3-3 proteins, thereby inhibiting FOXO transcriptional activity (7, 8). In a similar way, extracellular signal-regulated protein kinase (Erk) interacts with and phosphorylates FoxO3a promoting its degradation by an ubiquitin-proteasome pathway (13). On the other hand, FOXO factors and 14-3-3 proteins can also be phosphorylated by c-Jun N-terminal kinase (JNK), a member of the MAPK family activated by a variety of stress stimuli, including changes in levels of reactive oxygen species (ROS) (14, 15). This phosphorylation events lead to the release of FOXO from 14-3-3 chaperones and to the nuclear relocalization and activation of FOXO proteins (16, 17). Nuclear FOXO proteins trigger

apoptosis by modulating the expression of prodeath members of the Bcl-2 family, such as PUMA (18, 19).

Interferons (IFNs), particularly interferon-alpha (IFN-α), have been extensively used in the treatment of patients infected with hepatitis B or C virus. Since IFN-α appears to have antiproliferative effects on hepatocytes (20), it has been suggested that IFN-α therapy can prevent the subsequent development of HCC. There are several clinical studies that demonstrate that IFN-α therapy significantly improves the long-term survival and lowers the incidence of HCC among patients with chronic hepatitis C (21–27).

IFN-α is a member of the type I IFN family of glycoproteins, produced and secreted by the cells of the immune system in response to viral infection and/or tumour cells. This natural cytokine has multiple functions besides its antiviral properties, including modulation of immune responses and regulation of cell growth arrest and cell death (28–31). In addition, IFN-α has antitumour activity against a variety of tumours, although its greater efficacy has been reported in haematologic malignancies (32–35). The antitumour action of IFN-α might be conducted by indirect mechanisms such as immunomodulatory response (36–38) and antiangiogenic effects (39, 40), or by direct action on tumour cells inducing downregulation of oncogenes, expression of tumour suppressor genes and promoting apoptosis (41, 42). Although IFN-α has been shown to induce apoptosis in tumour cells, the molecular mechanisms mediating programmed cell death in response to this cytokine are not yet fully understood. We have already demonstrated *in vivo* that IFN-α2b treatment induces apoptosis of hepatic preneoplastic foci through a mechanism that involves hepatocyte production of ROS and secretion of transforming growth factor β1 (TGF-β1) (43–45). Moreover, we have shown that IFN-α2b triggers the mitochondrial apoptotic pathway (46). In addition, we showed that the Wnt/β-catenin/TCF pathway, a signalling mechanism associated with cancer, is activated at a very early stage of the development of the hepatocarcinogenic process and *in vivo* IFN-α2b treatment inhibits this pathway and promotes programmed cell death enhancing FOXO transcriptional activity (47).

In the present study, we went deeper on the study of the post-translational signal events triggered by the oxidative stress induced by IFN-α2b treatment and on the modulation of FoxO3a transcriptional activity during these events in preneoplastic rat livers.

Materials and methods

Chemicals

Diethylnitrosamine (DEN), 2-acetylaminofluorene (2-AAF), and ascorbic acid (ASC) were obtained from Sigma Chemical Co. (St. Louis, MO, USA). IFN-α2b was kindly provided by PC-Gen S.A. (Buenos Aires, Argentina). Anti-β-catenin antibody was from BD Transduction Labs (San Jose, CA, USA). Anti-Akt, anti-JNK, anti-p-JNK (T183/Y185), anti-Erk1/2 and anti-p-Erk1/2 (T202/Y204) antibodies were from Cell Signalling Technology (Danvers, MA, USA). Anti-pi class of rat glutathione S-transferase (rGST-P) antibody was purchased from Stressgen Bioreagents (Ann Arbor, MI, USA). Anti-FoxO3a, anti-p-FoxO3a (S253), anti-PUMAα/β, anti-p-Akt (S473), anti-Bax, anti-Bcl-x_L, anti-cytochrome c, anti-Histone H1 and anti-β-actin antibodies were from Santa Cruz Biotechnology (Santa Cruz, CA, USA). Antiprohibitin antibody was from Abcam (Cambridge, MA, USA). Pierce enhanced chemiluminescence (ECL™) Western Blotting Substrate was from Thermo Fisher Scientific (Rockford, IL, USA). Phosphatase inhibitor calyculin A was from BioSource International (Camarillo, CA, USA). All other chemicals were of the highest grade commercially available.

Animals and treatment

Adult male Wistar rats weighing 330–380 g were maintained in a room at constant temperature with a 12 h light–dark cycle, with food and water supplied *ad libitum*. Experimental protocols were performed according to the NIH 'Guide for the Care and Use of Laboratory Animals' (Publication no. 25–28, revised 1996). Animals were divided into three groups. An overview of the experimental protocol is provided in Figure 1. Animals of the initiated–promoted (IP) group were subjected to a two-phase model of rat hepatocarcinogenesis, as previously described (43). Briefly, animals received two intraperitoneal necrogenic doses of DEN (150 mg/kg body weight) 2 weeks apart. One week after the last injection of DEN, rats received 20 mg/kg body weight of 2-AAF by gavage for four consecutive days per week during 3 weeks. IP+IFN group was subjected to the same two-phase protocol as IP group and also received IFN-α2b (6.5×10^5 U/kg body weight), administered intraperitoneally three times per week during the entire treatment. The dose used was comparable to that used for therapeutic purposes (43). Animals from IP+IFN+ASC group, in addition to the two-phase protocol and IFN-α2b administration, received ASC (75 mg/kg body weight), administered intraperitoneally three times per week during the entire treatment. At the end of the 6-week treatment, animals were anesthetized and sacrificed and livers were removed and processed. At that time, approximately 5% of the liver is occupied by reversible preneoplastic foci (43).

Preparation of tissue lysates, homogenates and subcellular fractions

Whole liver lysates were prepared by homogenization of tissues in radioimmunoprecipitation assay buffer (RIPA,

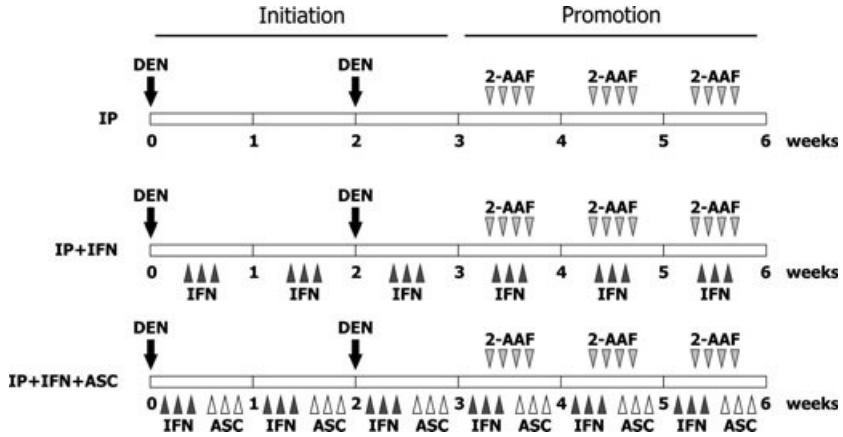

Fig. 1. Scheme for animal treatment. Male Wistar rats were subjected to a two-phase model of hepatocarcinogenesis. IP group received two intraperitoneal doses of DEN (150 mg/kg body weight) 2 weeks apart. One week after the last injection of DEN, the animals received 20 mg/kg body weight of 2-AAF by *gavage* for four consecutive days per week during 3 weeks. IP+IFN group was subjected to the same two-phase protocol and also received intraperitoneal IFN-α2b (6.5×10^5 U/kg body weight) three times per week during the entire treatment. IP+IFN+ASC animals were subjected to the hepatocarcinogenic treatment, also receiving IFN-α2b (6.5×10^5 U/kg body weight) and ASC (75 mg/kg body weight) three times per week during the entire treatment. Animals were sacrificed at the end of week 6.

20 mM Tris, pH 8, 200 mM NaCl, 1% Triton X-100, 1% sodium deoxycholate, 0.1% sodium dodecyl sulfate, 5 mM EDTA, 1 mM NaF, 1 mM Na_3VO_4, 1.5 nM Calyculin A and protease inhibitors), followed by three freeze-thawing cycles. Finally, tissue and cell debris were removed by centrifugation at 15 000 rpm for 30 min. Whole liver homogenates were prepared by homogenization of tissues in 0.3 M sucrose containing phosphatase inhibitors and protease inhibitors. For nuclear extracts preparation, whole liver homogenate was spin at 1000*g* for 10 min and the pellet was incubated in RIPA buffer at 4°C for 1 h (48). Finally, samples were centrifuged for 15 min at 8000*g* and supernatants were collected as the nuclear extracts. For cytosolic fractions preparation, whole liver homogenate was spin at 1000*g* for 10 min and the supernatant was centrifuged at 3300*g* for 10 min. The obtained supernatant was further centrifuged at 45 000 rpm for 1 h to collect the cytosolic fraction. Mitochondrial fractions were isolated by centrifugation of liver homogenates at 6000*g* for 15 min, washed and resuspended in 0.3 M sucrose containing phosphatase and protease inhibitors.

Assay for lipid peroxidation

Tissue lipid hydroperoxides (LPO) generation was considered as an indirect measure of ROS production. The amount of aldehydic products generated by lipid peroxidation in the liver homogenates was quantified by the thiobarbituric acid (TBA) reaction according to the spectrophotometric method of Ohkawa *et al.* (49) and measured by high-performance liquid chromatography (HPLC) with modifications introduced by *Young & Trimble* (50). The amount of thiobarbituric acid reactive substances (TBARS) was expressed as percentage of IP group.

Caspase 3 activity assay

The activity of caspase 3 was determined using an Enz-Chek caspase-3 assay kit (Molecular Probes, Eugene, OR, USA). The tissues were homogenized in lysis buffer (10 mM Tris, 200 mM NaCl, 1 mMEDTA and 0.001% Triton X-100) and, after differential centrifugation, the cytosolic fraction from each sample was used according to the manufacturer's instructions. Fluorescence was measured at an excitation wavelength of 360 nm and an emission wavelength of 465 nm in a DTX 880 Multimode Detector (Beckman Coulter, Brea, CA, USA).

Immunohistochemical assay

Liver tissues were fixed in 10% vol/vol formalin solution and embedded in low-melting paraffin blocks. Sections of 5 μm thickness were deparaffinized, rehydrated and then microwaved in a 10 mM citrate buffer solution for 10 min at 96°C to perform antigen retrieval. After incubation with blocking serum (3% BSA, 0.03% Triton X-100) for 30 min, slides were incubated with primary antibodies in a humidified chamber at 4°C overnight. For determination of preneoplastic foci, rGST-P immunodetection was chosen since it is the most widely used method for identification of altered hepatic foci (51). Consecutive slides were incubated with anti-rGST-P (dilution 1:100) or FoxO3a (dilution 1:10).primary antibodies. Detection of bound antibody was accomplished by the peroxidase-antiperoxidase method (52). Sections were counterstained with haematoxylin. Representative tissue images were captured from each experimental group using a digital camera (Q-Color5, Olympus America, Center Valley, PA, USA) attached to an inverted microscope (Axiovert 25, Zeiss, Göttingen, Germany). Slides were also stained in the absence of

primary antibodies to evaluate nonspecific secondary antibodies reactions.

Immunoblotting

Equal amounts of proteins were resolved on 12% SDS-polyacrilamide gels and transferred to polyvinylidene difluoride (PVDF) membranes (PerkinElmer Life Sciences Inc., Boston, MA, USA). Membranes were blocked with PBS-10% nonfat milk for 60 min, washed and incubated overnight at 4°C with primary antibody. Finally, membranes were incubated with peroxidase-conjugated secondary antibody and bands were detected by the ECL™ detection system and quantified by densitometry using the Gel-Pro Analyzer (Media Cybernetics, Silver Spring, MD, USA) software. Both equal loading and protein transfer for each membrane were checked by incubations with the proper antibodies and by Ponceau S staining.

Co-immunoprecipitation assay

Whole liver homogenates were subjected to immunoprecipitation with anti-β-catenin antibody (dilution 1:50). Proteins bound to protein A-sepharose beads were washed with lysis buffer and resolved by electrophoresis on 12% SDS-polyacrilamide gels. Gels were blotted onto PVDF membranes and subjected to immunoblotting with specific secondary antibody at appropriate dilution. The immunoreactive bands were detected as described above.

Protein concentration determination

The protein concentration was determined by the Lowry method (53), using bovine serum albumin as a standard.

RNA isolation and semiquantitative RT-PCR

PUMA mRNA expression was assayed by semiquantitative reverse transcription polymerase chain reaction (sqRT-PCR). Total RNA was isolated from rat liver tissues by the TriZOL method (Life Technologies Inc, Gaithersburg, MD, USA). Two μg of total RNA was used to prepare cDNA using an oligo-dT primer and M-MLV reverse transcriptase (Promega, Madison, WI, USA). Two μl of cDNA were amplified using Taq polymerase (Promega) and a specific set of primers. Amplification of mRNA transcript encoding β-actin, a housekeeping gene, was used as a quantitative control. See Table 1 for primers sequences and PCR conditions. PCR products were resolved in a 2% agarose gel stained with ethidium bromide and bands were visualized using a high-performance ultraviolet transilluminator (UVP, Upland, CA, USA). Images of the agarose gels were acquired with an imaging system EpiChemi 3 Darkroom (UVP) and quantification of the bands was performed using the Gel-Pro Analyser (Media Cybernetics, Silver Spring, MD, USA) software. Each quantified band was normalized to the corresponding β-actin levels.

Table 1. Primers used for PCR amplification

Primer*	Sequence 5′→3′	Cycles
β-actin F	CAACCTTCTTGCAGCTCCTC	30
β-actin R	TTCTGACCCATACCCACCAT	
PUMA F	CGTGTGGAGGAGGAGGAGT	36
PUMA R	TAGTTGGGCTCCATTTCTGG	

*Primer denominations refer to their target specificity and their sense (F, forward) or antisense (R, reverse) orientation. PCR conditions: reaction was started with a single step of denaturation at 95°C for 5 min. Cycling conditions consisted of denaturation at 95°C for 1 min, annealing at 55°C for 1 min, and extension at 72°C for 1 min. The PCR was finished with a 7 min, 72°C elongation step. In all cases, amplification was performed with the optimal conditions previously determined using an increasing number of PCR cycles. A linear relationship between the band intensity of the PCR product and the number of amplification cycles performed was observed. The conditions were chosen so that none of the amplification products reached a plateau at the end of the protocol.

Statistical analysis

Results were expressed as mean ± SEM. Significance in differences was tested by one-way ANOVA, followed by Tukey's test. Differences were considered significant when the P value was <0.05.

Results

Lipid peroxidation

We have examined the amount of LPO products, a marker of oxidative damage, by TBARS assay. TBARS levels are a reflection of the extent of oxidant status and are considered as an indicator of oxidative stress (54). As shown in Figure 2, TBARS levels in liver homogenates from IP+IFN animals were significantly higher than in those from IP group. On the other hand, TBARS levels in IP+IFN+ASC group were similar to those in IP group, without significant difference. It can be argued that IFN-α2b-induced ROS are responsible for the TBARS increment in IP+IFN group.

FoxO3a subcellular localization

FoxO3a protein levels were analysed in cytosolic and nuclear fractions by immunoblotting. Figure 3A shows that FoxO3a levels in cytosolic fractions were significantly decreased in IP+IFN compared with IP group. Conversely, in nuclear fraction, FoxO3a levels were significantly increased in IP+IFN compared with IP group (Fig. 3B). These effects were completely blocked in both subcellular fractions when animals were cotreated with ASC.

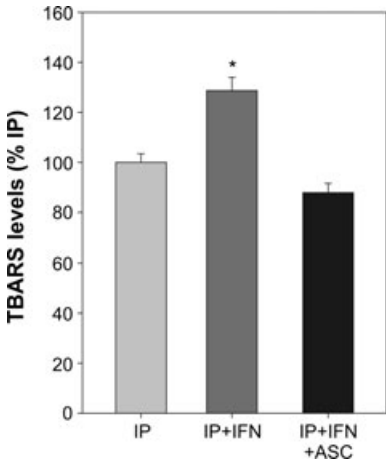

Fig. 2. Lipid peroxidation levels in liver homogenates determined by TBARS assay. IP: rats with hepatic preneoplasia, IP+IFN: IP rats that received IFN-α2b 6.5 × 10^5 U/kg body weight, IP+IFN+ASC: IP+IFN rats that also received ASC 75 mg/kg body weight. Results are expressed as percentages of IP group considered as 100% and are the mean ± SEM of five independent experiments. *$P < 0.05$ vs. IP.

In addition, FoxO3a localization was analysed by immunohistochemical staining. To examine the localization of FoxO3a within the preneplastic foci and in the surrounding tissue, rGST-P immunostaining was performed in consecutive slices. As seen in Figure 4, FoxO3a cytosolic staining was observed in all experimental groups, and no differences were observed between the preneoplastic lesions and the surrounding tissue. IP+IFN tissue shows weaker cytosolic FoxO3a staining than the other tissues. On the other hand, higher nuclear FoxO3a staining was visualized in IP+IFN liver tissue, mainly within the preneoplastic foci.

These results suggest that IFN-α2b-induced ROS stimulate FoxO3a shuttling from the cytosol to the nucleus.

Expression of activated JNK kinase

Since FoxO3a nuclear localization is favoured by JNK phosphorylation, we decided to measure the activation of JNK in total liver homogenates by immunoblotting. The analysis of the p-JNK:JNK ratio shows that phosphorylation of JNK was significantly elevated in IP+IFN group compared with IP group, whereas ASC cotreatment normalized this event (Fig. 5). These results suggest that ROS generated by IFN-α2b treatment are responsible for the activation of JNK.

Expression of activated Akt and Erk kinases

In an opposite manner to JNK, Akt phosphorylates FoxO3a in different specific residues of conserved domains and promotes the shuttling of this transcription factor from the nucleus to the cytosol where it is retained by 14-3-3 proteins (55). Additionally, Erk phosphorylates FoxO3a in a different set of specific residues enhancing its proteasome-mediated degradation (13). Hence, we analysed the presence of total Akt (Akt), activated Akt (p-Akt), total Erk (Erk1/2) and activated Erk (p-Erk1/2) in total liver homogenates by immunoblotting. Figure 6A shows that p-Akt:Akt ratio

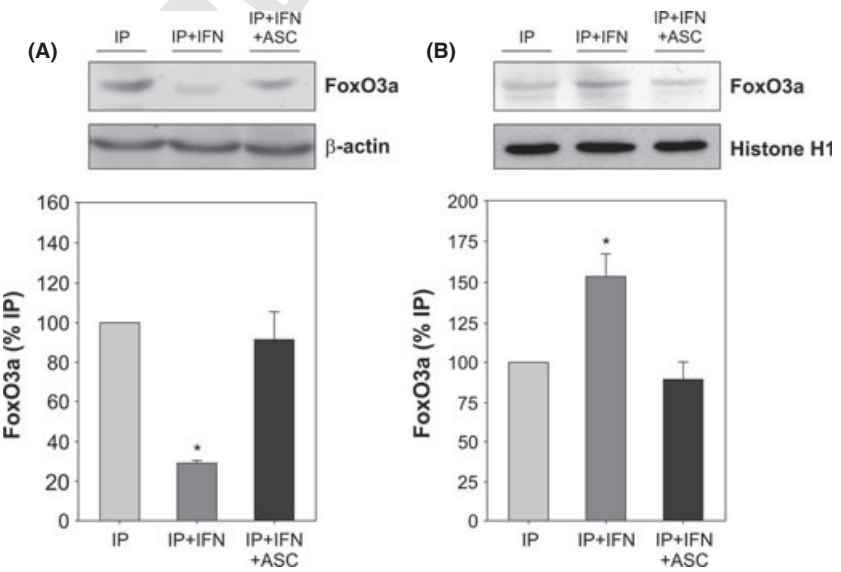

Fig. 3. Total FoxO3a protein expression in liver cytosolic (A) and nuclear (B) fractions. β-actin (A) and Histone H1 (B) were used as loading controls. IP: rats with hepatic preneoplasia, IP+IFN: IP rats that received IFN-α2b 6.5 × 10^5 U/kg body weight, IP+IFN+ASC: IP+IFN rats that also received ASC 75 mg/kg body weight. Densitometric analysis was performed and results are expressed as percentages of IP group considered as 100% and are the mean ± SEM of four independent experiments. *$P < 0.05$ vs. IP.

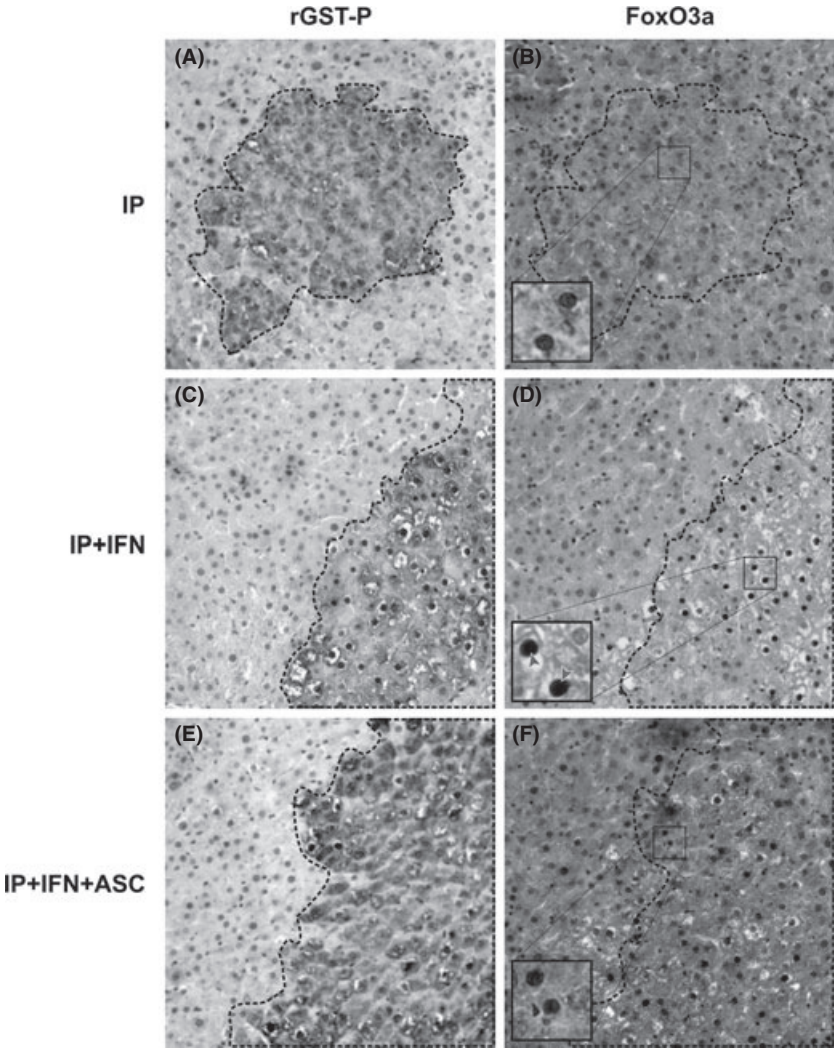

Fig. 4. Immunohistochemistry showing rGST-P-positive preneoplastic foci and subcellular localization of FoxO3a. Serial liver slices were immunostained with anti-rGST-P (A, C and E) or anti-FoxO3a (B, D and F). The nuclei were counterstained with haematoxylin. A, C and E: altered hepatic foci stained with anti-rGST-P antibody. B and F: IP and IP+IFN+ASC liver sections, respectively, showing cytosolic FoxO3a staining. D: IP+IFN liver sections showing both cytosolic and nuclear (arrowheads) FoxO3a staining. Original magnification 10x. Zoom magnification 40x. Livers were obtained from IP rats (A and B), IP+IFN rats (C and D) and IP+IFN+ASC rats (E and F). IP: rats with hepatic preneoplasia, IP+IFN: IP rats that received IFN-α2b 6.5×10^5 U/kg body weight, IP+IFN+ASC: IP+IFN rats that also received ASC 75 mg/kg body weight.

was significantly decreased in IP+IFN and IP+IFN+ASC groups compared with IP group. Figure 6B shows that p-Erk1/2:Erk1/2 ratio was significantly decreased in IP+IFN group compared with IP group. In addition, p-Erk1/2:Erk1/2 ratio for IP+IFN+ASC group shows no significant difference respect to IP group. These results suggest that IFN-α2b treatment blocks Akt and Erk activation during the onset of hepatic preneoplasia. Moreover, the effects of IFN- α2b on the activation of Akt are independent of ROS.

FoxO3a phosphorylation by Akt

We analysed total FoxO3a and FoxO3a specifically phosphorylated by Akt (p-Foxo3a) in total liver lysates. Figure 7 shows that p-FoxO3a:FoxO3a ratio was significantly decreased in IP+IFN and IP+IFN+ASC groups compared with IP group. These results are in agreement with those obtained for the active form of Akt.

β-catenin/TCF4 vs. β-catenin/FoxO3a association

Nuclear FoxO3a can act as a transcriptional factor regulating a group of specific target genes. It was reported that FOXO transcriptional activity is enhanced by association with the cofactor β-catenin and this interaction is favoured under oxidative stress conditions (17, 56). We have previously reported in preneoplastic livers the activation of the Wnt canonical pathway, which involves the protein β-catenin and the transcriptional factor

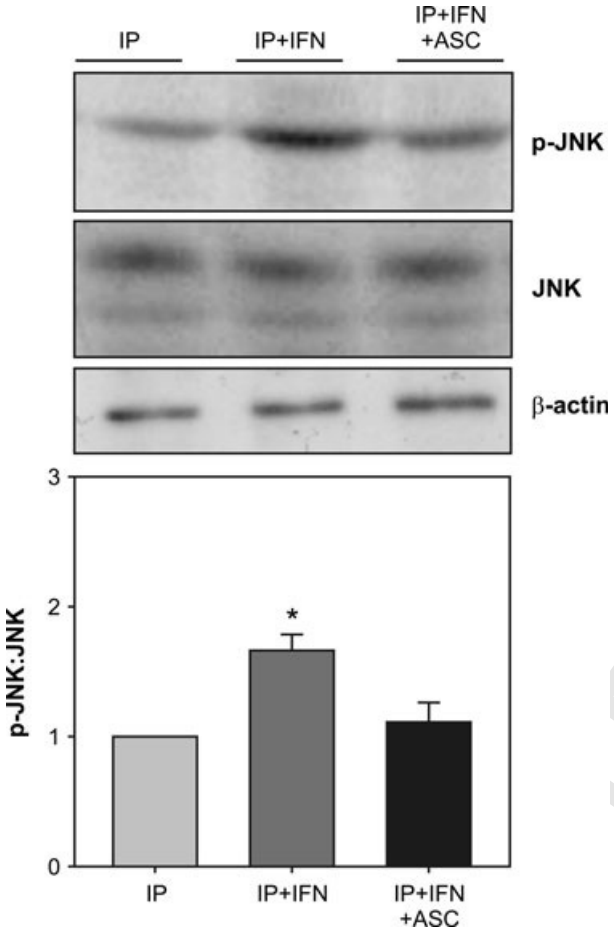

Fig. 5. Activation of JNK kinase. JNK activation was evaluated by immunoblotting in total liver homogenates with antibodies against active JNK (p-JNK) and total JNK (JNK). β-actin was used as loading control. IP: rats with hepatic preneoplasia, IP+IFN: IP rats that received IFN-α2b 6.5 × 10^5 U/kg body weight, IP+IFN+ASC: IP+IFN rats that also received ASC 75 mg/kg body weight. Densitometric analysis was performed and means ± SEM of four independent experiments were calculated. Results are expressed as the ratio p-JNK:JNK relative to IP group considered as 1. *$P < 0.05$ vs. IP.

TCF4 (47). Co-immunoprecipitation assay was performed to evaluate the dual role of β-catenin as a cofactor of TCF4 and FoxO3a and the effects of ROS in these interactions. Figure 8 shows that β-catenin/FoxO3a association was favoured in oxidative conditions as seen in IP+IFN group, in an opposite manner to β-catenin/TCF4 association.

Expression of PUMA, an apoptosis related FoxO3a target gene

FoxO3a modulates the transcription of several genes involved in the mitochondria-dependent and -independent apoptotic process. PUMA is one of the proapoptotic members of the Bcl-2 family regulated by FoxO3a and is exclusively controlled at a transcriptional level, whereas other members can be modulated by multiple mechanisms (57). For this reason, we measured the transcription levels of mRNA encoding PUMA by sqRT-PCR method and mitochondrial protein levels of PUMAα/β by immunoblotting. Figure 9A shows that PUMA mRNA levels were significantly higher in IP+IFN group compared with IP group. ASC cotreatment totally blocked this increase, leading to PUMA mRNA levels comparable to IP group. Similar results were obtained when PUMA protein levels were analysed in mitochondrial fractions, as seen in Figure 9B.

Analysis of apoptotic events

We have previously demonstrated that *in vivo* IFN-α2b treatment increases apoptosis on rat hepatic preneoplastic foci (43, 45). On a regular basis, apoptotic cells are checked by haematoxylin/eosin staining in liver sections, and apoptotic index (AI) is morphologically determined as well. In the present work, the obtained AI revealed similar results to those determined by this and other methods (43, 45). AI values within AHF of IP+IFN group were two-fold higher than those for IP and IP+IFN+ASC groups (data not shown). Furthermore, we have demonstrated that this apoptotic process involves an increase in the mitochondrial Bax protein (43). Since the fate of the cells is largely dependent on the Bax:Bcl-x_L ratio, here we analysed this by immunoblotting. We observed that the mitochondrial Bax:Bcl-x_L ratio was significantly increased in IP+IFN compared with IP group. Treatment with ASC reduced the ratio to values similar to those in IP group (Fig. 10A).

It is well-known that Bax translocation to the mitochondrial membrane promotes its homodimerization that finally conducts to cell death by disruption of the mitochondrial membrane, release of cytochrome c to the cytosol and subsequent activation of caspase-3. Therefore, we analysed the release of cytochrome c to cytosolic fractions by immunoblotting. Figure 10B shows that cytochrome c levels were significantly higher in IP+IFN group compared with IP group. ASC cotreatment totally blocked this increase, obtaining cytochrome c levels comparable to IP group.

In addition, we analysed caspase-3 activity, as its activation is the ultimate responsible for the majority of the apoptotic effects. The analysis of caspase-3 activity (Fig. 10C) shows a significant higher activity in IP+IFN group compared with IP group. By contrast, cotreatment with ASC resulted in a decreased caspase-3 activity, reaching similar levels to IP group. In addition, we also observed a decrease in the protein level of procaspase-3 (inactive caspase-3 precursor) in IP+IFN group (Figure 10D).

Discussion

FoxO3a is a member of the FoxO subfamily of Forkhead transcription factors and is well-known as an important

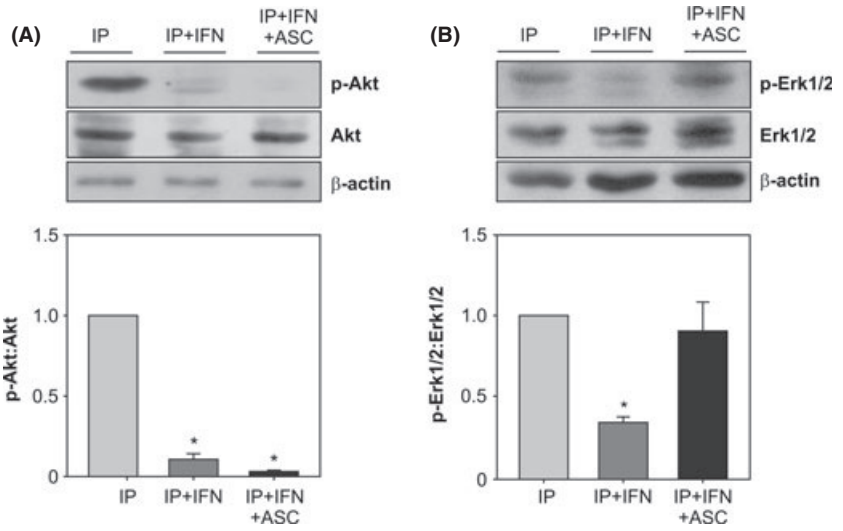

Fig. 6. Activation of Akt and Erk kinases. Akt and Erk activations were evaluated by immunoblotting in total liver homogenates with antibodies against active Akt (p-Akt), total Akt (Akt), active Erk1/2 (p-Erk1/2) and total Erk1/2 (Erk1/2). β-actin was used as loading control. IP: rats with hepatic preneoplasia, IP+IFN: IP rats that received IFN-α2b 6.5 × 10^5 U/kg body weight, IP+IFN+ASC: IP+IFN rats that also received ASC 75 mg/kg body weight. Densitometric analysis was performed and means ± SEM of four independent experiments were calculated. Results are expressed as the ratios p-Akt:Akt or pErk1/2:Erk1/2 relatives to IP group considered as 1. **P* < 0.05 vs. IP.

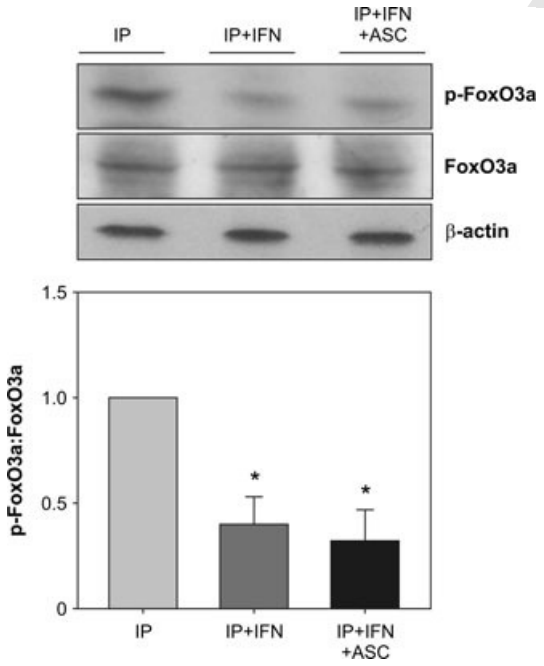

Fig. 7. Akt-phosphorylated FoxO3a protein expression. FoxO3a specifically phosphorylated by Akt (p-FoxO3a) was evaluated by immunoblotting in total liver lysates with antibodies against phosphorylated FoxO3a (p-FoxO3a) and total FoxO3a (FoxO3a). β-actin was used as loading control. IP: rats with hepatic preneoplasia, IP+IFN: IP rats that received IFN-α2b 6.5 × 10^5 U/kg body weight, IP+IFN+ASC: IP+IFN rats that also received ASC 75 mg/kg body weight. Densitometric analysis was performed and means ± SEM of four independent experiments were calculated. Results are expressed as the ratio p-FoxO3a:FoxO3a relative to IP group considered as 1. **P* < 0.05 vs. IP.

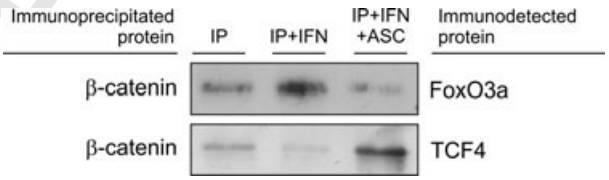

Fig. 8. β-catenin, TCF4 and FoxO3a co-immunoprecipitation assay. Immunoprecipitated and immunodetected proteins are indicated in the figure. IP: rats with hepatic preneoplasia, IP+IFN: IP rats that received IFN-α2b 6.5 × 10^5 U/kg body weight, IP+IFN+ASC: IP+IFN rats that also received ASC 75 mg/kg body weight.

regulator of apoptosis. For this reason, identifying ways to activate FoxO3a protein during the early stages of the carcinogenic process may be critical to eliminate preneoplastic cells and avoid tumour progression.

In a previous work, we have reported that *in vivo* IFN-α2b treatment on preneoplastic rat livers attenuates the Wnt/β-catenin/TCF pathway in a process involving FoxO3a transcription factor (47). We have also proved that IFN-α2b induces the production of ROS in primary culture of hepatocytes from preneoplastic livers by activation of the membrane bound NADPH oxidase complex (45). In addition, we have presented compelling evidence that these IFN-α2b-induced ROS act as an intracellular messenger triggering the apoptotic process observed in altered hepatic foci (45).

Prompted by this evidence, we have tested herein the hypothesis that *in vivo* IFN-α2b treatment in preneoplastic livers promotes the activation of FoxO3a in a mechanism mediated by ROS, and that this transcription factor may be responsible for the attenuation of the

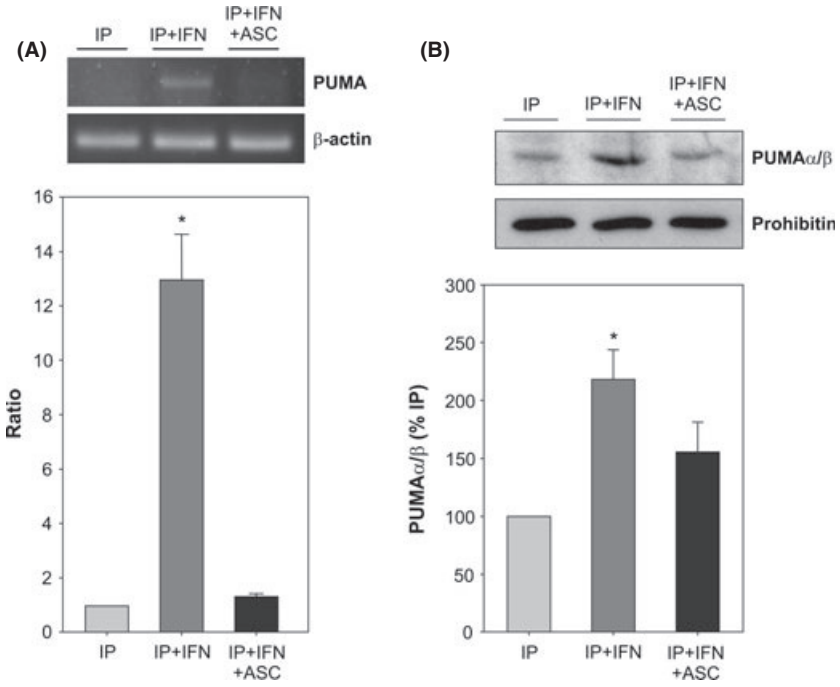

Fig. 9. PUMA mRNA and protein expression. (A) Expression levels of PUMA mRNA transcript by sqRT-PCR. Densitometric analysis was performed in four independent experiments. Intensity of the bands was quantified and normalized to the corresponding β-actin levels. Ratios are presented in a graphical form and indicate the relative level of the amplification product over the IP sample after normalization to the housekeeping gene and are the mean ± SEM of three independent experiments. (B) PUMAα/β protein expression in liver mitochondrial fraction by immunoblotting. Densitometric analysis was performed and results are expressed as percentages of IP group considered as 100%, and are the mean ± SEM of six independent experiments. IP: rats with hepatic preneoplasia, IP+IFN: IP rats that received IFN-α2b 6.5×10^5 U/kg body weight, IP+IFN+ASC: IP+IFN rats that also received ASC 75 mg/kg body weight. *$P < 0.05$ vs. IP.

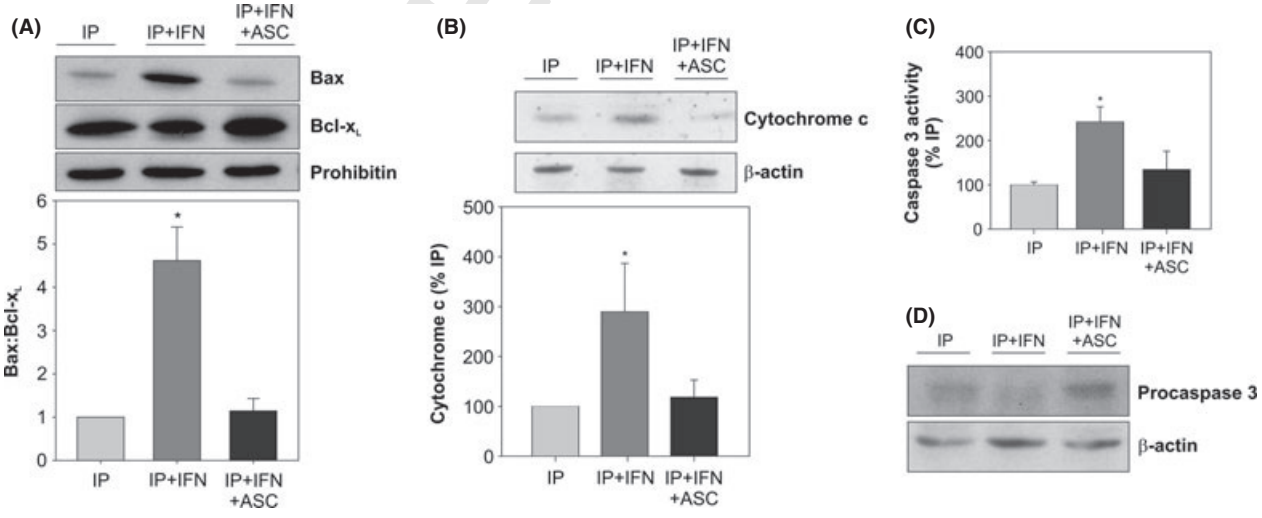

Fig. 10. Analysis of apoptosis markers. (A) Study of Bax and Bcl-xL mitochondrial levels by immunoblotting. Densitometric analyses were performed and Bax:Bcl-xL ratio was calculated. Results are expressed as relative to IP group considered as 1, and are means ± SEM of three independent experiments. (B) Expression levels of cytochrome c in liver cytosolic fractions by immunoblotting. Densitometric analysis was performed and results are expressed as percentages of IP group and are the mean ± SEM of four independent experiments. (C) The activity of caspase 3 was determined by a fluorometric assay. The bars represent caspase 3 activity, expressed in percentage and considering IP group as 100%. Data are expressed as means ± SEM of four independent experiments. (D) A representative image of procaspase 3 analysis by immunoblotting showing a decrease in IP+IFN group. IP: rats with hepatic preneoplasia, IP+IFN: IP rats that received IFN-α2b 6.5×10^5 U/kg body weight, IP+IFN+ASC: IP+IFN rats that also received ASC 75 mg/kg body weight. *$P < 0.05$ vs. IP.

Wnt/β-catenin pathway and the increased apoptotic process in the preneoplastic lesions.

First, we evaluated the oxidative status of the livers from animals subjected to the experimental protocols measured by TBARS assay. Preneoplastic livers from animals treated with IFN-α2b presented significantly higher oxidative stress than preneoplastic livers. We also observed that oxidative stress levels in preneoplastic livers treated with IFN-α2b and ASC were similar to those of the IP group, suggesting that the dose of ASC used was sufficient to reduce ROS generated by the IFN-α2b treatment.

Functional activity of FOXO transcription factors are tightly regulated at a post-translational level mainly by reversible modifications such as phosphorylations. This signal-induced events control FOXOs subcellular localization and protein stability. According to their phosphorylation profile, FOXOs can shuttle between the nucleus and the cytosol. In the nucleus, FOXOs are transcriptionally active and control the transcription of genetic programs involved in several processes including programmed cell death. When FOXOs are located in the cytosol, they become transcriptionally inactive and can undergo proteolytic degradation. The phosphorylation events mentioned above are conducted particularly by JNK, Akt and Erk kinases. JNK and Akt kinases have opposite effects on the localization of FOXO proteins, whereas Erk kinase promotes FOXO degradation. In the present study, we found that Akt was active in preneoplastic livers respect to control animals (data not shown), phosphorylating FoxO3a and promoting its sequestration in the cytosol. Since a constitutive activation of the PI3K/Akt pathway is a hallmark of many cancers and this process occurs at an early stage in the carcinogenic process, this finding was predictable in our preneoplastic model. Surprisingly, Akt activation was abolished in the other experimental groups, suggesting a mechanism that involves IFN-α2b but is not dependent of ROS. This result proposes a novel and unknown mechanism by which IFN-α2b inhibits Akt activation in preneoplastic livers. Further analysis would be necessary to deepen the mechanism of action of this cytokine on PI3K/Akt signalling pathway. For Erk, however, we found that *in vivo* IFN-α2b treatment inhibited Erk activation and cotreatment with ascorbic acid reactivated this kinase as measured by p-Erk1/2:Erk1/2 ratio. This inhibitory effect of IFN-α, including IFN-α2b, on the activation of Erk was already reported in HCC cell lines and other types of cell lines (58–60). In agreement with our results, the positive effect of ascorbic acid on the activation of Erk was reported by others (61, 62). On the other hand, we demonstrate that IFN-α2b-induced ROS are responsible for the activation of JNK which is known to promote the translocation of FoxO3a to the nucleus. Our results demonstrate that IFN-α2b-induced ROS improves FoxO3a nuclear translocation.

Once in the nucleus, FOXOs recognize consensus sequences in the DNA and upregulate a set of target genes, including the BH3-only protein PUMA (18, 19). PUMA is an important mediator of the apoptotic process and is induced in a p53-dependent and –independent manner (63). You *et al.* have reported that FoxO3a upregulates PUMA expression when PI3K/Akt signalling is downregulated (18). In agreement, we found a significant increase of PUMA, both at mRNA and protein levels, in IFN-α2b-treated preneoplastic livers. In addition, ASC treatment completely blocked these increments providing evidence that IFN-α2b-induced ROS are involved in the nuclear localization and transcriptional activation of FoxO3a. PUMA is a proapoptotic player that interacts with the antiapoptotic members of the Bcl-2 family, releasing proapoptotic members of the same family such as Bax. Bax homodimerization is followed by mitochondrial membrane disruption. After this, cytochrome c is released from the mitochondria into the cytosol where it participates in caspases activation. In accordance with the upregulation of PUMA, we found in IP+IFN group a significant increase of the Bax: Bcl-x_L ratio, a higher release of cytochrome c and an increase in caspase 3 activity. In addition, we also found an inhibition of these events in IP+IFN+ASC group, compared with IP group.

It was reported that an evolutionarily conserved interaction exists between β-catenin and FOXO proteins (56). Moreover, FOXO transcriptional activity was enhanced when β-catenin/FOXO interaction was favoured by oxidative stress conditions (56). In the present and also in a previous work (47), we found in IFN-α2b-treated preneoplastic livers that FoxO3a presented higher affinity for β-catenin than TCF. This event led to the dissociation of β-catenin from TCF, which acted as a transactivator of this transcription factor. As a consequence, TCF activity was repressed and the pathway was no longer actived as we previously proved by sqRT-PCR of several target genes of TCF (47).

In summary, we proved that *in vivo* IFN-α2b treatment induced nuclear translocation and transcriptional activity of FoxO3a, further confirming that the external manipulation of the oxidative cell environment is key to the carcinogenic process and is an useful tool to define therapeutic strategies.

Acknowledgements

The authors thank PC-Gen S.A. for the generous gift of recombinant IFN-α2b. This work was supported by Research Grant PICT 05-38068 (MC Carrillo) from Agencia Nacional de Promoción Científica y Tecnológica (ANPCyT), by Consejo Nacional de Investigaciones Científicas y Técnicas (CONICET, PIP No. 1246 2009-2011) and by Instituto Nacional del Cáncer (INC, Grant No. 8, MC Carrillo).

Conflict of interest: The authors do not have any disclosures to report. 5

References

1. Jemal A, Bray F, Center MM, *et al.* Global cancer statistics. *CA Cancer J Clin* 2011; **61**: 69–90.
2. Perz JF, Armstrong GL, Farrington LA, Hutin YJ, Bell BP. The contributions of hepatitis B virus and hepatitis C virus infections to cirrhosis and primary liver cancer worldwide. *J Hepatol* 2006; **45**: 529–38.
3. Nordenstedt H, White DL, El-Serag HB. The changing pattern of epidemiology in hepatocellular carcinoma. *Dig Liver Dis* 2010; **42**(Suppl. 3): S206–14.
4. Biggs WH 3rd, Cavenee WK, Arden KC. Identification and characterization of members of the FKHR (FOX O) subclass of winged-helix transcription factors in the mouse. *Mamm Genome* 2001; **12**: 416–25.
5. Jacobs FM, van der Heide LP, Wijchers PJ, *et al.* FoxO6, a novel member of the FoxO class of transcription factors with distinct shuttling dynamics. *J Biol Chem* 2003; **278**: 35959–67.
6. Furuyama T, Nakazawa T, Nakano I, Mori N. Identification of the differential distribution patterns of mRNAs and consensus binding sequences for mouse DAF-16 homologues. *Biochem J* 2000; **349**(Pt 2): 629–34.
7. Biggs WH 3rd, Meisenhelder J, Hunter T, Cavenee WK, Arden KC. Protein kinase B/Akt-mediated phosphorylation promotes nuclear exclusion of the winged helix transcription factor FKHR1. *Proc Natl Acad Sci USA* 1999; **96**: 7421–6.
8. Brunet A, Bonni A, Zigmond MJ, *et al.* Akt promotes cell survival by phosphorylating and inhibiting a Forkhead transcription factor. *Cell* 1999; **96**: 857–68.
9. Kops GJ, Burgering BM. Forkhead transcription factors: new insights into protein kinase B (c-akt) signaling. *J Mol Med (Berl)* 1999; **77**: 656–65.
10. Nakae J, Park BC, Accili D. Insulin stimulates phosphorylation of the forkhead transcription factor FKHR on serine 253 through a Wortmannin-sensitive pathway. *J Biol Chem* 1999; **274**: 15982–5.
11. Rena G, Guo S, Cichy SC, Unterman TG, Cohen P. Phosphorylation of the transcription factor forkhead family member FKHR by protein kinase B. *J Biol Chem* 1999; **274**: 17179–83.
12. Tang ED, Nuñez G, Barr FG, Guan KL. Negative regulation of the forkhead transcription factor FKHR by Akt. *J Biol Chem* 1999; **274**: 16741–6.
13. Yang JY, Zong CS, Xia W, *et al.* ERK promotes tumorigenesis by inhibiting FOXO3a via MDM2-mediated degradation. *Nat Cell Biol* 2008; **10**: 138–48.
14. Vlahopoulos S, Zoumpourlis VC. JNK: a key modulator of intracellular signaling. *Biochemistry (Mosc)* 2004; **69**: 844–54.
15. Shen HM, Liu ZG. JNK signaling pathway is a key modulator in cell death mediated by reactive oxygen and nitrogen species. *Free Radic Biol Med* 2006; **40**: 928–39.
16. Sunayama J, Tsuruta F, Masuyama N, Gotoh Y. JNK antagonizes Akt-mediated survival signals by phosphorylating 14-3-3. *J Cell Biol* 2005; **170**: 295–304.
17. Essers MA, Weijzen S, de Vries-Smits AM, *et al.* FOXO transcription factor activation by oxidative stress mediated by the small GTPase Ral and JNK. *EMBO J* 2004; **23**: 4802–12.
18. You H, Pellegrini M, Tsuchihara K, *et al.* FOXO3a-dependent regulation of Puma in response to cytokine/growth factor withdrawal. *J Exp Med* 2006; **203**: 1657–63.
19. Amente S, Zhang J, Lavadera ML, *et al.* Myc and PI3K/AKT signaling cooperatively repress FOXO3a-dependent PUMA and GADD45a gene expression. *Nucleic Acids Res* 2011; **39**: 9498–507.
20. Radaeva S, Jaruga B, Hong F, *et al.* Interferon-alpha activates multiple STAT signals and down-regulates c-Met in primary human hepatocytes. *Gastroenterology* 2002; **122**: 1020–34.
21. Nishiguchi S, Kuroki T, Nakatani S, *et al.* Randomised trial of effects of interferon-alpha on incidence of hepatocellular carcinoma in chronic active hepatitis C with cirrhosis. *Lancet* 1995; **346**: 1051–5.
22. Sata M, Ide T, Akiyoshi F, *et al.* Effects of interferon alpha 2a on incidence of hepatocellular carcinoma in chronic active hepatitis without cirrhosis. Hepatitis Treatment Study Group. *Kurume Med J* 1997; **44**: 171–7.
23. Tanaka H, Tsukuma H, Kasahara A, *et al.* Effect of interferon therapy on the incidence of hepatocellular carcinoma and mortality of patients with chronic hepatitis C: a retrospective cohort study of 738 patients. *Int J Cancer* 2000; **87**: 741–9.
24. Mazzella G, Accogli E, Sottili S, *et al.* Alpha interferon treatment may prevent hepatocellular carcinoma in HCV-related liver cirrhosis. *J Hepatol* 1996; **24**: 141–7.
25. Tanaka K, Sata M, Uchimura Y, Suzuki H, Tanikawa K. Long-term evaluation of interferon therapy in hepatitis C virus-associated cirrhosis: does IFN prevent development of hepatocellular carcinoma? *Oncol Rep* 1998; **5**: 205–8.
26. Shiratori Y, Ito Y, Yokosuka O, *et al.* Antiviral therapy for cirrhotic hepatitis C: association with reduced hepatocellular carcinoma development and improved survival. *Ann Intern Med* 2005; **142**: 105–14.
27. Omata M, Yoshida H, Shiratori Y. Prevention of hepatocellular carcinoma and its recurrence in chronic hepatitis C patients by interferon therapy. *Clin Gastroenterol Hepatol* 2005; **3**(10 Suppl 2): S141–3.
28. Pestka S, Langer JA, Zoon KC, Samuel CE. Interferons and their actions. *Annu Rev Biochem* 1987; **56**: 727–77.
29. Pestka S, Krause CD, Walter MR. Interferons, interferon-like cytokines, and their receptors. *Immunol Rev* 2004; **202**: 8–32.
30. Stark GR, Kerr IM, Williams BR, Silverman RH, Schreiber RD. How cells respond to interferons. *Annu Rev Biochem* 1998; **67**: 227–64.
31. Pfeffer LM. Biologic activities of natural and synthetic type I interferons. *Semin Oncol* 1997; **24**(3 Suppl 9): S9-63–9.
32. Gutterman JU. Cytokine therapeutics: lessons from interferon alpha. *Proc Natl Acad Sci USA* 1994; **91**: 1198–205.
33. Goldstein D, Laszlo J. The role of interferon in cancer therapy: a current perspective. *CA Cancer J Clin* 1988; **38**: 258–77.
34. Gresser I. Wherefore interferon? *J Leukoc Biol* 1997; **61**: 567–74.
35. Morris A, Zvetkova I. Cytokine research: the interferon paradigm. *J Clin Pathol* 1997; **50**: 635–9.
36. Gresser I. Antitumour effects of interferons: past, present and future. *Br J Haematol* 1991; **79**(Suppl. 1): 1–5.
37. Gresser I, Kaido T, Maury C, *et al.* Interaction of IFN alpha/beta with host cells essential to the early inhibition

of Friend erythroleukemia visceral metastases in mice. *Int J Cancer* 1994; **57**: 604–11.
38. Kaido TJ, Maury C, Gresser I. Host CD4 + T lymphocytes are required for the synergistic action of interferon-alpha/beta and adoptively transferred immune cells in the inhibition of visceral ESb metastases. *Cancer Res* 1995; **55**: 6133–9.
39. Sidky YA, Borden EC. Inhibition of angiogenesis by interferons: effects on tumor- and lymphocyte-induced vascular responses. *Cancer Res* 1987; **47**: 5155–61.
40. Dinney CP, Bielenberg DR, Perrotte P, *et al.* Inhibition of basic fibroblast growth factor expression, angiogenesis, and growth of human bladder carcinoma in mice by systemic interferon-alpha administration. *Cancer Res* 1998; **58**: 808–14.
41. Ferrantini M, Capone I, Belardelli F. Interferon-alpha and cancer: mechanisms of action and new perspectives of clinical use. *Biochimie* 2007; **89**: 884–93.
42. Chawla-Sarkar M, Lindner DJ, Liu YF, *et al.* Apoptosis and interferons: role of interferon-stimulated genes as mediators of apoptosis. *Apoptosis* 2003; **8**: 237–49.
43. de Luján Alvarez M, Cerliani JP, Monti J, *et al.* The in vivo apoptotic effect of interferon alfa-2b on rat preneoplastic liver involves Bax protein. *Hepatology* 2002; **35**: 824–33.
44. de Luján Alvarez M, Ronco MT, Ochoa JE, *et al.* Interferon alpha-induced apoptosis on rat preneoplastic liver is mediated by hepatocytic transforming growth factor beta (1). *Hepatology* 2004; **40**: 394–402.
45. Quiroga AD, Alvarez Mde L, Parody JP, *et al.* Involvement of reactive oxygen species on the apoptotic mechanism induced by IFN-alpha2b in rat preneoplastic liver. *Biochem Pharmacol* 2007; **73**: 1776–85.
46. Alvarez Mde L, Quiroga AD, Ronco MT, *et al.* Time-dependent onset of Interferon-alpha2b-induced apoptosis in isolated hepatocytes from preneoplastic rat livers. *Cytokine* 2006; **6**: 245–53.
47. Parody JP, Alvarez ML, Quiroga AD, *et al.* Attenuation of the Wnt/beta-catenin/TCF pathway by in vivo interferon-alpha2b (IFN-alpha2b) treatment in preneoplastic rat livers. *Growth Factors* 2010; **28**: 166–77.
48. De Duve C, Pressman BC, Gianetto R, Wattiaux R, Appelmans F. Tissue fractionation studies. 6. Intracellular distribution patterns of enzymes in rat-liver tissue. *Biochem J* 1955; **60**: 604–17.
49. Ohkawa H, Ohishi N, Yagi K. Assay for lipid peroxides in animal tissues by thiobarbituric acid reaction. *Anal Biochem* 1979; **95**: 351–8.
50. Young IS, Trimble ER. Measurement of malondialdehyde in plasma by high performance liquid chromatography with fluorimetric detection. *Ann Clin Biochem* 1991; **28**(Pt 5): 504–8.
51. Pitot HC. Altered hepatic foci: their role in murine hepatocarcinogenesis. *Annu Rev Pharmacol Toxicol* 1990; **30**: 465–500.
52. Kaku T, Ekem JK, Lindayen C, *et al.* Comparison of formalin- and acetone-fixation for ummunohistochemical detection of carcinoembryonic antigen (CEA) and keratin. *Am J Clin Pathol* 1983; **80**: 806–15.
53. Lowry OH, Rosebrough NJ, Farr AL, Randall RJ. Protein measurement with the Folin phenol reagent. *J Biol Chem* 1951; **193**: 265–75.
54. Wen JJ, Yachelini PC, Sembaj A, Manzur RE, Garg NJ. Increased oxidative stress is correlated with mitochondrial dysfunction in chagasic patients. *Free Radic Biol Med* 2006; **41**: 270–6.
55. Tzivion G, Dobson M, Ramakrishnan G. FoxO transcription factors; Regulation by AKT and 14-3-3 proteins. *Biochim Biophys Acta* 2011; **1813**: 1938–45.
56. Essers MA, de Vries-Smits LM, Barker N, *et al.* Functional interaction between beta-catenin and FOXO in oxidative stress signaling. *Science* 2005; **308**: 1181–4.
57. Yu J, Zhang L. PUMA, a potent killer with or without p53. *Oncogene* 2008; **27**(Suppl. 1): S71–83.
58. Inamura K, Matsuzaki Y, Uematsu N, *et al.* Rapid inhibition of MAPK signaling and anti-proliferation effect via JAK/STAT signaling by interferon-alpha in hepatocellular carcinoma cell lines. *Biochim Biophys Acta* 2005; **1745**: 401–10.
59. Li C, Chi S, He N, *et al.* IFNalpha induces Fas expression and apoptosis in hedgehog pathway activated BCC cells through inhibiting Ras-Erk signaling. *Oncogene* 2004; **23**: 1608–17.
60. Romerio F, Riva A, Zella D. Interferon-alpha2b reduces phosphorylation and activity of MEK and ERK through a Ras/Raf-independent mechanism. *Br J Cancer* 2000; **83**: 532–8.
61. Park S, Park CH, Hahm ER, *et al.* Activation of Raf1 and the ERK pathway in response to l-ascorbic acid in acute myeloid leukemia cells. *Cell Signal* 2005; **17**(1): 111–9.
62. Temu TM, Wu KY, Gruppuso PA, Phornphutkul C. The mechanism of ascorbic acid-induced differentiation of ATDC5 chondrogenic cells. *Am J Physiol Endocrinol Metab* 2010; **299**: E325–34.
63. Jeffers JR, Parganas E, Lee Y, *et al.* Puma is an essential mediator of p53-dependent and -independent apoptotic pathways. *Cancer Cell* 2003; **4**: 321–8.

Author Query Form

Journal: LIV
Article: 12421

Dear Author,
During the copy-editing of your paper, the following queries arose. Please respond to these by marking up your proofs with the necessary changes/additions. Please write your answers on the query sheet if there is insufficient space on the page proofs. Please write clearly and follow the conventions shown on the attached corrections sheet. If returning the proof by fax do not write too close to the paper's edge. Please remember that illegible mark-ups may delay publication.
Many thanks for your assistance.

Query reference	Query	Remarks
1	**AUTHOR: A running head short title was not supplied; please check if this one is suitable and, if not, please supply a short title of up to 40 characters that can be used instead.**	
2	**AUTHOR: It is the journal style to abbreviate the author(s) middle name. Only the first name and surname should be spelt in full. Please check all the author names and indicate which is the first name, middle name and surname. Eg: Michael Cornelius Abrams should be changed to Michael C. Abrams if Cornelius is the middle name.**	
3	**AUTHOR: 15 000 rpm: please replace this with the correct *g* value.**	
4	**AUTHOR: 45 000 rpm: please replace this with the correct *g* value.**	
5	**AUTHOR: Please check and confirm if they have any conflict of interest to declare.**	

USING e-ANNOTATION TOOLS FOR ELECTRONIC PROOF CORRECTION

Required software to e-Annotate PDFs: Adobe Acrobat Professional or Adobe Reader (version 8.0 or above). (Note that this document uses screenshots from Adobe Reader X)
The latest version of Acrobat Reader can be downloaded for free at: http://get.adobe.com/reader/

Once you have Acrobat Reader open on your computer, click on the Comment tab at the right of the toolbar:

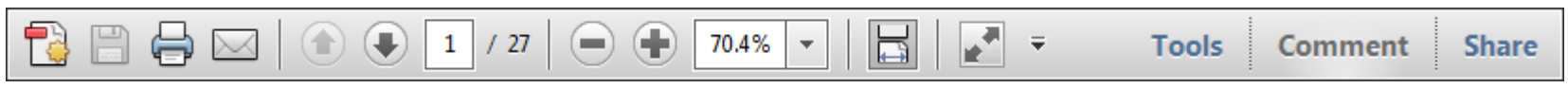

This will open up a panel down the right side of the document. The majority of tools you will use for annotating your proof will be in the Annotations section, pictured opposite. We've picked out some of these tools below:

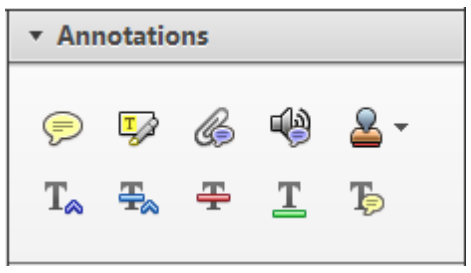

1. Replace (Ins) Tool – for replacing text.

Strikes a line through text and opens up a text box where replacement text can be entered.

How to use it

- Highlight a word or sentence.
- Click on the Replace (Ins) icon in the Annotations section.
- Type the replacement text into the blue box that appears.

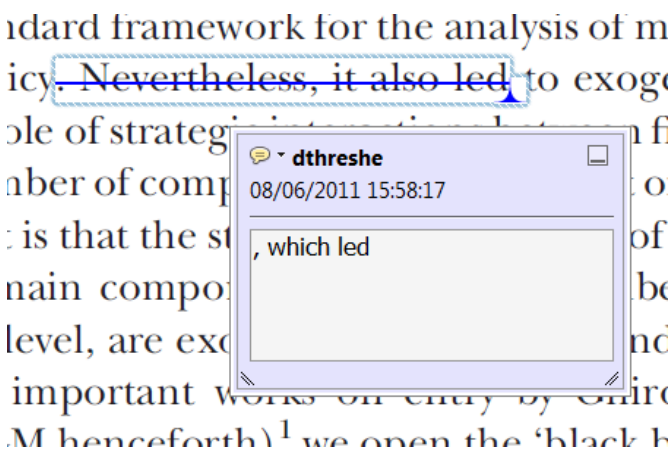

2. Strikethrough (Del) Tool – for deleting text.

Strikes a red line through text that is to be deleted.

How to use it

- Highlight a word or sentence.
- Click on the Strikethrough (Del) icon in the Annotations section.

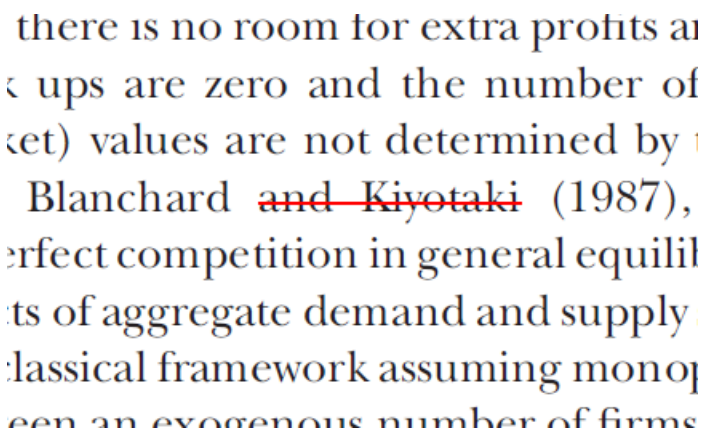

3. Add note to text Tool – for highlighting a section to be changed to bold or italic.

Highlights text in yellow and opens up a text box where comments can be entered.

How to use it

- Highlight the relevant section of text.
- Click on the Add note to text icon in the Annotations section.
- Type instruction on what should be changed regarding the text into the yellow box that appears.

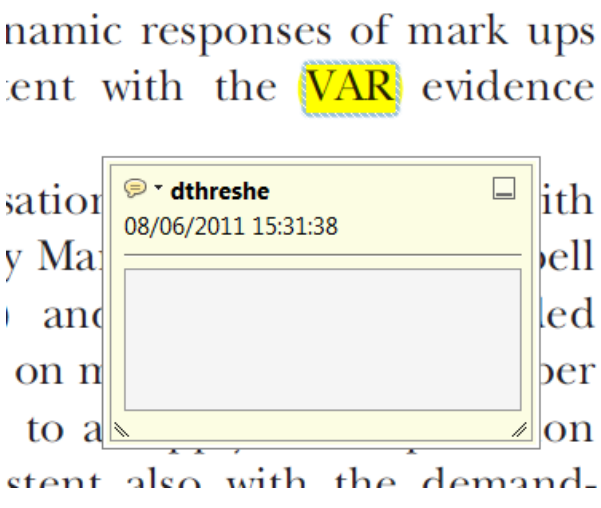

4. Add sticky note Tool – for making notes at specific points in the text.

Marks a point in the proof where a comment needs to be highlighted.

How to use it

- Click on the Add sticky note icon in the Annotations section.
- Click at the point in the proof where the comment should be inserted.
- Type the comment into the yellow box that appears.

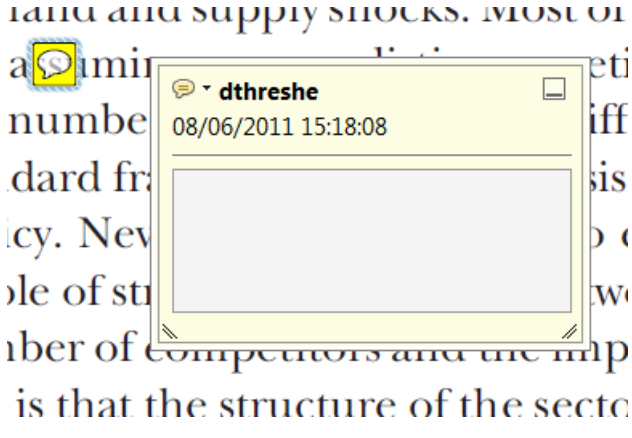

WILEY-BLACKWELL

USING e-ANNOTATION TOOLS FOR ELECTRONIC PROOF CORRECTION

5. Attach File Tool – for inserting large amounts of text or replacement figures.

Inserts an icon linking to the attached file in the appropriate pace in the text.

How to use it

- Click on the Attach File icon in the Annotations section.
- Click on the proof to where you'd like the attached file to be linked.
- Select the file to be attached from your computer or network.
- Select the colour and type of icon that will appear in the proof. Click OK.

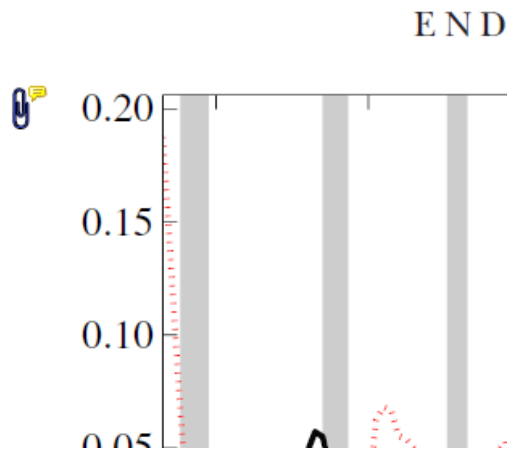

6. Add stamp Tool – for approving a proof if no corrections are required.

Inserts a selected stamp onto an appropriate place in the proof.

How to use it

- Click on the Add stamp icon in the Annotations section.
- Select the stamp you want to use. (The Approved stamp is usually available directly in the menu that appears).
- Click on the proof where you'd like the stamp to appear. (Where a proof is to be approved as it is, this would normally be on the first page).

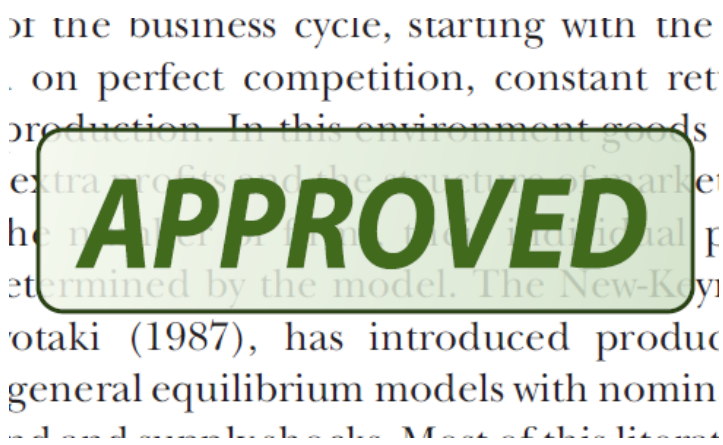

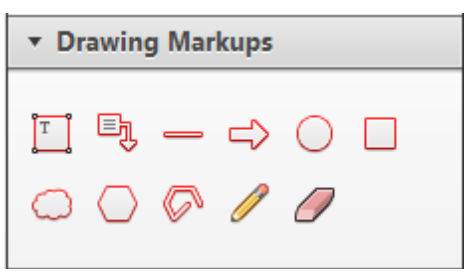

7. Drawing Markups Tools – for drawing shapes, lines and freeform annotations on proofs and commenting on these marks.

Allows shapes, lines and freeform annotations to be drawn on proofs and for comment to be made on these marks..

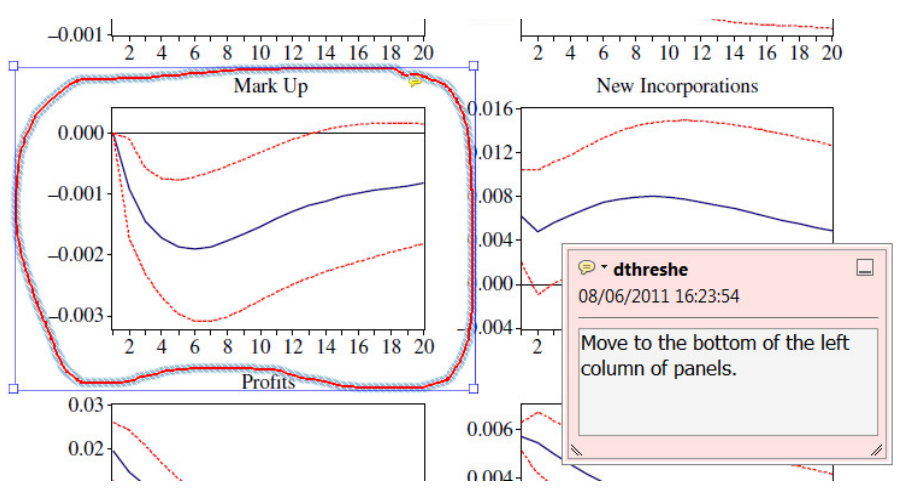

How to use it

- Click on one of the shapes in the Drawing Markups section.
- Click on the proof at the relevant point and draw the selected shape with the cursor.
- To add a comment to the drawn shape, move the cursor over the shape until an arrowhead appears.
- Double click on the shape and type any text in the red box that appears.

For further information on how to annotate proofs, click on the Help menu to reveal a list of further options: